

Energy densities of magnetic field and relativistic electrons at the innermost region of the M87 jet

M. Kino^{1,a}, F. Takahara², K. Hada^{3,4}, and A. Doi¹

¹ISAS/JAXA, 3-1-1 Yoshinodai, Chuo, Sagami-hara 252-5210, Japan

²Department of Earth and Space Science, Osaka University, Toyonaka 560-0043, Japan

³INAF/IRA, via Gobetti 101, I-40129 Bologna, Italy

⁴NAOJ, Osawa, Mitaka, Tokyo 181-8588, Japan

Abstract. We explore energy densities of magnetic fields and relativistic electrons in M87 jet. Since the radio core at the base of the M87 jet is the optically thick surface against synchrotron self absorption (SSA), observations directly give the size and turnover frequency for SSA. Using the observed angular diameter 0.11 mas, which corresponds to 16 Schwarzschild radii of the central black hole with 6×10^9 solar mass, and the flux density of the radio core at 43 GHz, we estimate the energy densities of magnetic field (U_B) and relativistic electrons (U_e) by comparing the standard SSA formula to the observed radio core. Together with the allowed total kinetic power of the M87 jet, we find that (i) the allowed B is limited in the range $2 \text{ G} \leq B \leq 13 \text{ G}$, and that (ii) $0.18 \leq U_e/U_B \leq 66$ holds. Our results significantly constrain formation mechanism of relativistic jets in active galactic nuclei.

1 Introduction

Formation mechanism of relativistic jets in active galactic nuclei (AGNs) remains as a longstanding unresolved problem in astrophysics. Although an importance of estimations of magnetic field energy density (U_B) and electron one (U_e) for resolving the formation mechanism had been emphasized (e.g., [13]; [5]), it is not observationally clear whether U_B or U_e is dominant at a jet base. Deviation from equi-partition (i.e., $U_e/U_B \approx 1$) is essential for investigation of relativistic jet formation. However, no one has succeeded in firmly obtaining a robust estimation of an actual value of U_e/U_B at a jet base.

M87, a nearby giant radio galaxy located at a distance of $D = 16.7$ Mpc, hosts one of the most massive super massive black hole $M_\bullet = (3 - 6) \times 10^9 M_\odot$ and thus M87 is the best source for investigating a jet base. Furthermore, M87 has been well studied at wavelength from radio to Very High Energy (VHE) γ -ray ([1] and reference therein) and causality arguments based on VHE γ -ray outburst in February 2008 indicate that the VHE emission region is less than $\sim 5\delta R_s$ where δ is the relativistic Doppler factor ([2]). VLBA beam resolution at 43GHz typically attains about 0.21×0.43 mas which is equivalent to $5.3 \times 10^{16} \times 1.1 \times 10^{17}$ cm. If we take $M_\bullet = 6 \times 10^9 M_\odot$, then VLBA beam resolution corresponds to $30 \times 60 R_s$. Recent progress of VLBI observations reveals the innermost structure of the M87 jet, i.e., frequency and core-size relation, distance and core-size relation down to close to 16 Schwarzschild radii (R_s) ([12], hereafter H11). Thus,

^ae-mail: kino@vsop.isas.jaxa.jp

the jet base of M87 is the best laboratory for investigation of U_e/U_B in a real vicinity of a central engine.

Two significant forward steps are recently obtained in M87 observations and the present work is motivated by them. (1) H11 succeed in directly measuring core-shift phenomena at the jet base of M87 at 2, 5, 8, 15, 22 and 43 GHz. The radio core position at each frequency has been obtained by the astrometric observation of the core shift along the M87 jet. Since the radio core surface corresponds to the optically-thick surface at each frequency, a synchrotron-self-absorption (SSA) turnover frequency ν_{ssa} is identical to the observed frequency itself. (2) We recently measure core sizes in [10] (hereafter H13). Hereafter we focus on the radio core at 43GHz. In H13, we select VLBA data observed after 2009 with sufficiently good qualities (all 10 stations participated and good uv-coverages). To measure the width of the core, a single, full-width-half-maximum (FWHM) Gaussian is fitted for observed core in the perpendicular direction to the jet axis and we derive the width of the core (θ_{FWHM}). We stress that the core width is free from the uncertainty of viewing angle. Therefore, using θ_{FWHM} at 43GHz, we can estimate model-independent value of U_e/U_B in the 43GHz core of M87 for the first time.

2 One-zone Model

Here, we derive the explicit expression of U_e/U_B by using the fundamental formula of SSA process ([9], hereafter GS65; [4], hereafter BG70; [21], hereafter RL79). Two

physical quantities, B and K_e are determined by the comparison of physical quantities measured by VLBA observations (i.e., θ_{obs} , $\nu_{\text{ssa,obs}}$, and $S_{\nu_{\text{ssa,obs}}}$) and standard SSA process. In this work, we define the radio spectral index α as $S_\nu \propto \nu^{-\alpha}$.

Following assumptions are adopted in this work:

- We assume uniform and isotropic distribution of relativistic electrons in the radio core at 43 GHz (the hatched circle in Fig. 1). For M87, polarized flux seems not very large. Therefore, we assume isotropic tangled magnetic field in this work. Hereafter, we denote B as the magnetic field strength perpendicular to the direction of electron motion. Then, the total field strength is given by $B_{\text{tot}} = \sqrt{3}B$.
- We assume the emission region is spherical with its radius R measured at the comoving frame. The radius is defined as $2R = \theta_{\text{obs}}D$ where D is the distance to a source. There might be a slight difference between θ_{FWHM} and θ_{obs} . VLBI measured θ_{FWHM} is conventionally treated as $\theta_{\text{obs}} = \theta_{\text{FWHM}}$, while [17] (hereafter M83) pointed out a deviation expressed as $\theta_{\text{obs}} \approx 1.8\theta_{\text{FWHM}}$ which is caused by a forcible fitting of Gaussians to a non-Gaussian component. In this work, we introduce a factor A defined as $\theta_{\text{obs}} \equiv A\theta_{\text{FWHM}}$ and $1 \leq A \leq 1.8$ is assumed.

At the radio core, (1) $\tau_{\text{ssa}} = 1$ at $\nu = \nu_{\text{ssa}}$ holds:

$$\tau_{\nu_{\text{ssa}}} = 2\alpha_{\nu_{\text{ssa}}}R = 1, \quad (1)$$

where $\tau_{\nu_{\text{ssa}}}$, and $\alpha_{\nu_{\text{ssa}}}$ are the optical depth for SSA, and the absorption coefficient for SSA, respectively. The optically thin emission equals the optically thick one at ν_{ssa} :

$$\frac{4\pi}{3}R^3\epsilon_{\nu_{\text{ssa}}} = 4\pi R^2 S_{\nu_{\text{ssa}}}, \quad (2)$$

where $\epsilon_{\nu_{\text{ssa}}}$, and $S_{\nu_{\text{ssa}}}$ are the emissivity and flux per unit frequency, respectively. Via these two relations, we can solve B and K_e .

The term K_e , the normalization factor of electron number density distribution $n_e(\gamma)$, is defined as

$$n_e(\gamma_e)d\gamma_e = K_e\gamma_e^{-p}d\gamma_e \quad (\gamma_{e,\text{min}} \leq \gamma_e \leq \gamma_{e,\text{max}}), \quad (3)$$

where $p = 2\alpha + 1$, $\gamma_{e,\text{min}}$, and $\gamma_{e,\text{max}}$ are a spectral index, a minimum Lorentz factor, and a maximum Lorentz factor of relativistic electrons, respectively. Let us further review optically thin synchrotron emissions. The maximum in the spectrum of synchrotron radiation from an electron occurs at the frequency: (Eq. 2.23 in GS65)

$$\nu_{\text{syn}} = 1.2 \times 10^6 B \gamma_e^2 \quad (4)$$

where B is the component of magnetic field perpendicular to the direction of the electron motion.

3 Results

Obtained expressions for B and K_e are as follows;

$$B = b(p) \left(\frac{\nu_{\text{ssa,obs}}}{1 \text{ GHz}} \right)^5 \left(\frac{\theta_{\text{obs}}}{1 \text{ mas}} \right)^4 \left(\frac{S_{\nu_{\text{ssa,obs}}}}{1 \text{ Jy}} \right)^{-2} \times \left(\frac{\delta}{1+z} \right) \quad (5)$$

and

$$K_e = k(p) \left(\frac{\nu_{\text{ssa,obs}}}{1 \text{ GHz}} \right)^{-2p-3} \left(\frac{D}{1 \text{ Gpc}} \right)^{-1} \left(\frac{\theta_{\text{obs}}}{1 \text{ mas}} \right)^{-2p-5} \times \left(\frac{S_{\nu_{\text{ssa,obs}}}}{1 \text{ Jy}} \right)^{p+2} \left(\frac{\delta}{1+z} \right)^{-p-3}, \quad (6)$$

where the numerical coefficients $b(p)$ and $k(p)$ are shown in M83 and [15]. From the above expressions, we can obtain the ratio U_e/U_B explicitly as

$$\begin{aligned} \frac{U_e}{U_B} &= \left(\frac{B_{\text{tot}}^2}{8\pi} \right)^{-1} \int_{\gamma_{e,\text{min}}}^{\gamma_{e,\text{max}}} \gamma_e m_e c^2 n_e(\gamma_e) d\gamma_e \\ &= \frac{8\pi m_e c^2}{3(p-2)} \frac{k(p)\gamma_{\text{min}}^{-p+2}}{b^2(p)} \left(\frac{\nu_{\text{ssa,obs}}}{1 \text{ GHz}} \right)^{-2p-13} \left(\frac{D}{1 \text{ Gpc}} \right)^{-1} \\ &\times \left(\frac{\theta_{\text{obs}}}{1 \text{ mas}} \right)^{-2p-13} \left(\frac{S_{\nu_{\text{ssa,obs}}}}{1 \text{ Jy}} \right)^{p+6} \left(\frac{\delta}{1+z} \right)^{-p-5} \\ &\text{(for } p > 2\text{)}. \end{aligned} \quad (7)$$

From this, we can estimate U_e/U_B without minimum energy (equipartition B field) assumption. It is clear that the measurement of θ_{obs} is crucial for determining U_e/U_B . We argue details on it in the next subsection. It is also evident that a careful treatment of $\gamma_{e,\text{min}}$ is crucial for determining U_e/U_B ([14]).

To evaluate realistic U_e/U_B , we should take realistic parameter ranges. To this end, we take into uncertainty into account.

Regarding α , a simultaneous observation of the spectrum measurement at sub-mm wavelength range is crucial, since most of the observed fluxes at sub-mm range come from the innermost part of the jet. It has been indeed measured by [8] with multi-frequency ALMA observation (cycle 0) and it is robust that $\alpha > 0.5$ at > 200 GHz where synchrotron emission becomes optically-thin against SSA.

As for allowed θ_{obs} , we set

$$0.11 \text{ mas} \leq \theta_{\text{obs}} \leq 0.20 \text{ mas}, \quad (8)$$

where we use the average value $\theta_{\text{FWHM}} = 0.11$ mas from H13 and maximum of θ_{obs} is $0.11 \text{ mas} \times 1.8 = 0.198$ mas.

The maximal value of $\gamma_{e,\text{min}}$ can be estimated with $\theta_{\text{obs}} = 0.20$ mas. Allowed ranges of $\gamma_{e,\text{min}}$ is given by $1 \leq \gamma_{e,\text{min}} \leq 2 \times 10^2$, here we set maximum value of $\gamma_{e,\text{min}}$ by requiring synchrotron emission is produced at least above 43 GHz. We further impose a condition that time-averaged bulk kinetic power as inferred from its large-scale radio and X-ray morphology L_{jet} should be smaller than the power at the 43GHz core

$$\begin{aligned} L_{\text{jet}} &\geq \max[L_{\text{poy}}, L_e], \\ L_e &= \frac{4\pi}{3} \Gamma^2 \beta R^2 c U_e \\ L_{\text{poy}} &= \frac{4\pi}{3} \Gamma^2 \beta R^2 c U_B, \end{aligned} \quad (9)$$

where L_{jet} at large-scale is estimated to be a few $\times 10^{44}$ ergs $^{-1}$ (e.g., [20]). Hereafter, we assume $\Gamma\beta = 1$ for simplicity and a slight deviation from this does not influence the main results in this work. Regarding L_{jet} in the

M87 jet, we set $5 \times 10^{44} \text{ ergs}^{-1} \leq L_{\text{jet}} \leq 3 \times 10^{45} \text{ ergs}^{-1}$ where upper limit of L_{jet} includes an uncertainty due to the deviation from time-averaged L_{jet} at while flaring phenomena at the jet base may temporally increase L_{jet} . X-ray light curve at the M87 core over 10 years showed a flux variation by a factor of ~ 6 except for exceptionally high X-ray flux during giant VHE flares which happened in 2008 and 2010 (Fig. 1 in [1]). Based on it, we allow the largest jet kinetic power case as $L_{\text{jet}} = 6 \times 5 \times 10^{44} \text{ ergs}^{-1} = 3 \times 10^{45} \text{ ergs}^{-1}$. In this work, we demonstrate the case of $L_{\text{jet}} = 3 \times 10^{45} \text{ ergs}^{-1}$.

In Fig. 2, we show the allowed $\log(U_e/U_B)$ as a function of $\gamma_{e,\text{min}}$ and B with $L_{\text{jet}} = 3 \times 10^{45} \text{ erg s}^{-1}$ and $p = 3.5$. Note that the field strength B has one-to-one correspondence to θ_{obs} . From Fig. 2, one can see that the absolute value of B (equivalent to θ_{obs}) is more dominant factor than $\gamma_{e,\text{min}}$ in this allowed ranges. We find that energy density of relativistic electrons dominates over the one of magnetic field ($\log(U_e/U_B) > 1$) when $B < 5.7 \text{ G}$ and vice versa. The larger $\gamma_{e,\text{min}}$ leads to smaller $\log(U_e/U_B)$ because U_e becomes smaller for larger $\gamma_{e,\text{min}}$. The allowed $\gamma_{e,\text{min}}$ is limited in $30 \leq \gamma_{e,\text{min}} \leq 2 \times 10^2$. The smallest U_e/U_B realizes at $B \approx 8.1 \text{ G}$ and it is $U_e/U_B = 0.18$. The allowed U_e/U_B is governed by the limit of $L_j \geq \max[L_{\text{poy}}, L_e]$. The lower part of $\log(U_e/U_B)$ is determined by the condition of $L_e = L_j$, while the upper part is settled by $L_{\text{poy}} = L_j$. The largest U_e/U_B is realized when $B = 2.5 \text{ G}$ which shows $U_e/U_B = 66$.

4 Summary and discussions

Based on VLBA observation data at 43 GHz, we explore U_e/U_B at the base of the M87 jet. We use standard basic theory of synchrotron radiation with the simplest geometry of one-zone sphere model for the radio core at 43 GHz. We impose the upper limit of total jet power L_{jet} based on various previous works. We then find the following things;

- We obtain the allowed range of B as $2 \text{ G} < B < 13 \text{ G}$ in the observed radio core at 43GHz with its diameter 0.11 mas ($(16 R_s)$). Our estimate of B is basically close to the previous estimate in the literature (e.g., [19]), although fewer assumptions have been made in this work.

Our result excludes a strong magnetic field such as $B \sim 10^{3-4} \text{ G}$ which is frequently assumed in previous works in order to activate Blandford-Znajek process ([3]). Although M87 has been a prime target for testing relativistic MHD jet simulation studies powered by black-hole spin energy, our result provides a very stringent limit on the maximum B , one of the critical parameters in relativistic MHD jets model.

- We obtain the allowed region of U_e/U_B in the allowed θ_{obs} and $\gamma_{e,\text{min}}$ plane. The resultant U_e/U_B contains both the region of $U_e/U_B > 1$ and $U_e/U_B < 1$. What we should emphasize here is that the deviation from $U_e/U_B \approx 1$ is not very large. It is found that the allowed range is $0.18 \leq U_e/U_B \leq 66$.

This result gives a tight constraint against relativistic MHD models since they seem to postulate much larger

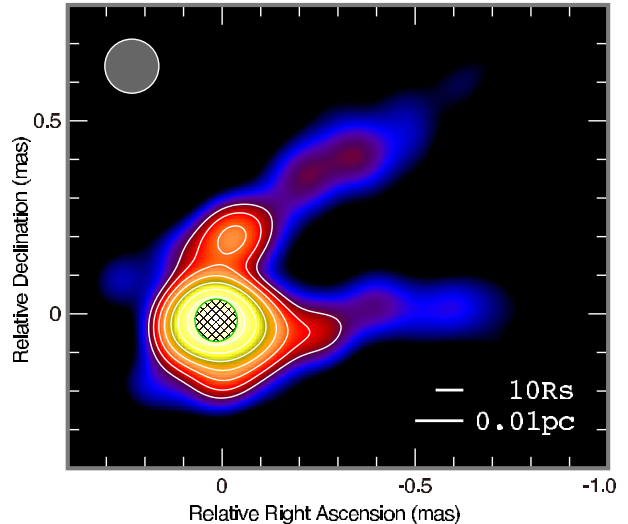


Figure 1. VLBA image of M87 at 43GHz. The the core width (i.e., length perpendicular to the jet axis) derived by the gaussian fitting by AIPS task "JMFIT" is $\theta_{\text{FWHM}} = 0.11 \text{ mas}$ (see details in H13). The hatched circle marks the 0.11 mas diameter region explored in this work. Contours start from 3σ image rms level and increasing by factors of 1.4.

U_B/U_e at a jet-base than the maximum value obtained in this work (e.g., [23]). For example, the jet flow is heavily Poynting dominated at the jet base with $U_B/U_e \sim 10^3$ in [18]. Therefore, the obtained U_e/U_B in this work gives a tight constraint on the initial conditions in relativistic MHD models.

Lastly, we briefly comment on key future works. Observationally, it is crucial to obtain resolved images the radio cores at 43GHz with space/sub-mm VLBI which would clarify whether there is a sub-structure or not inside $\sim 16 R_s$ scale at M87 jet base. Towards this observational final goal, as a first step, it is important to explore physical relations between the results of the present work and observational data at higher frequencies such as 86 GHz and 230 GHz (e.g., [16]; [7]). Indeed, we intend to conduct a new observation of M87 at 86 GHz and we will explore this issue using the new data. Space-VLBI program also could play key role since lower frequency observation can attain higher dynamic range images with a high resolution (e.g., [6]; [22]).

Acknowledgment

We thank A. Tchekhovskoy for useful discussions. This work is partially supported by Grant-in-Aid for Scientific Research, KAKENHI 24540240 (MK) and 24340042 (AD) from Japan Society for the Promotion of Science (JSPS).

References

- [1] Abramowski, A., Acero, F., Aharonian, F., et al. 2012, *ApJ*, **746**, 151
- [2] Acciari, V. A., et al. 2009, *Science*, **325**, 444

- [3] Blandford, R. D., & Znajek, R. L. 1977, MNRAS, **179**, 433
- [4] Blumenthal, G. R., & Gould, R. J. 1970, Reviews of Modern Physics, **42**, 237 (BG70)
- [5] Burbidge, G. R., Jones, T. W., & Odell, S. L. 1974, ApJ, **193**, 43
- [6] Dodson, R., Edwards, P. G., & Hirabayashi, H. 2006, PASJ, **58**, 243
- [7] Doeleman, S. S., Fish, V. L., Schenck, D. E., et al. 2012, Science, **338**, 355
- [8] Doi, A., Hada, K., Nagai, H., et al. 2013, this proceedings
- [9] Ginzburg, V. L., & Syrovatskii, S. I. 1965, ARA&A, **3**, 297 (GS65)
- [10] Hada, K., Kino, M., Doi, A., et al. 2013, ApJ, in press (H13)
- [11] Hada, K., Kino, M., Nagai, H., et al. 2012, ApJ, **760**, 52 (H12)
- [12] Hada, K., Doi, A., Kino, M., et al. 2011, Nature, **477**, 185 (H11)
- [13] Kellermann, K. I., & Pauliny-Toth, I. I. K. 1969, ApJL, **155**, L71
- [14] Kino, M., Takahara, F., & Kusunose, M. 2002, ApJ, **564**, 97
- [15] Kino, M., Takahara, F., Hada, K., & Doi, A. 2013, *in preparation*
- [16] Krichbaum, T. P., Graham, D. A., Bremer, M., et al. 2006, Journal of Physics Conference Series, **54**, 328
- [17] Marscher, A. P. 1983, ApJ, **264**, 296 (M83)
- [18] McKinney, J. C. 2006, MNRAS, **368**, 1561
- [19] Neronov, A., & Aharonian, F. A. 2007, ApJ, **671**, 85
- [20] Owen, F. N., Eilek, J. A., & Kassim, N. E. 2000, ApJ, **543**, 611
- [21] Rybicki, G. B., & Lightman, A. P. 1979, New York, Wiley-Interscience, 1979 (RL79)
- [22] Takahashi, R., & Mineshige, S. 2011, ApJ, **729**, 86
- [23] Tchekhovskoy, A., Narayan, R., & McKinney, J. C. 2011, MNRAS, **418**, L79

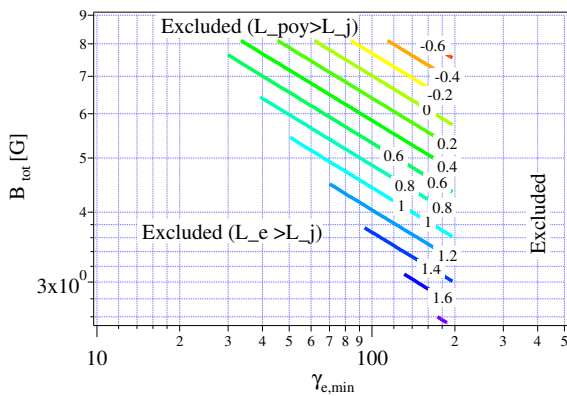


Figure 2. The energy density ratio of $\log(U_e/U_B)$ in the allowed $\gamma_{e,\min} - B$ plane with $L_j = 3 \times 10^{45} \text{ erg s}^{-1}$ and $p = 3.5$.